15th Australasian Fluid Mechanics Conference
The University of Sydney, Sydney, Australia
13-17 December 2004

Experimental-Numerical investigation of a bend diffuser-configuration

A.J. Simonsen[1] **and P.-Å. Krogstad**[2]

[1]Present address: SINTEF Energy Research, Energy Processes. Kolbjørn Hejes v. 1b, N-7065 Trondheim, Norway

[2]Department of Energy and Process Engineering, The Norwegian University of Science and Technology, N-7491 Trondheim, Norway

Abstract

The current work presents an experimental-numerical investigation of the flow in a special bend-diffuser configuration. Measured data of static pressure, time-mean velocity, and estimates of the skin friction are compared with the results from a numerical model. The main objective of the comparison was to obtain information on how well the numerical simulations using standard turbulence models, were able to reproduce the experimental data. Although the geometry is simple the combination of flow curvature and adverse pressure gradient generates complex flow physics.

Introduction

Intercooling between different compressor stages are commonly used to reduce compressor work and thereby increase the total efficiency of gas turbine cycles. Effective intercooling is partly achieved by reducing the fluid velocity after compressors using diffusers. Since flow in diffusers are subjected to an adverse pressure gradient there is a potential danger for flow separation to occur which could lead to loss in performance as well as damage of downstream equipment. The aim of design is to keep the adverse pressure gradient as high as possible, but below a critical limit, by controlling the length versus outlet/inlet area-ratio of the diffuser. The configuration described in the current paper is tailored for applications were axial compressors are used and allowable axial length is limited. The new configuration turns the axial flow outwards radially through a axial-to-radial bend. After the bend a small stabilizing section with constant flow area follows before the diffusion process starts. Radial diffusers are not uncommon, but their main application is after a centrifugal compressor which, considering the importance of inlet boundary conditions on diffuser performance, is a completely different flow configuration.

Experimental setup

Figure 1 shows a schematic view of the test rig. A centrifugal fan was used for air supply. The channels and settling chamber were made of galvanised plates while the models were made out of transparent plexiglass. Static pressure was measured with a linear response pressure transducer. The uncertainty of the static pressure measurements are within one percent. For the velocity measurements a $2.5\mu m$ Platinum-rhodium(90/10%) single hot-wire wire was used. The hot-wire was calibrated in a separate unit and moved to the test rig without disconnecting the cable. It was carefully put into the probe-holder and inclined with the horizontal direction using a level tool. Measurement accuracy for mean velocity, taking into account high turbulence intensity, probe misalignment and calibration errors, is estimated to be within 6%. The distance from the wall to the first measurement point was measured with a telescope mounted on a micrometer. The channel wall was polished and gave a reflected image of the probe giving an accuracy roughly estimated to be of order $0.1mm$. Later, the wall position was optimized with a wall function fit leading to a correction of the original value usually less than $0.1mm$. Figure 2 shows the different sections where velocity was measured and table 1 gives an overview of geometrical and flow related data.

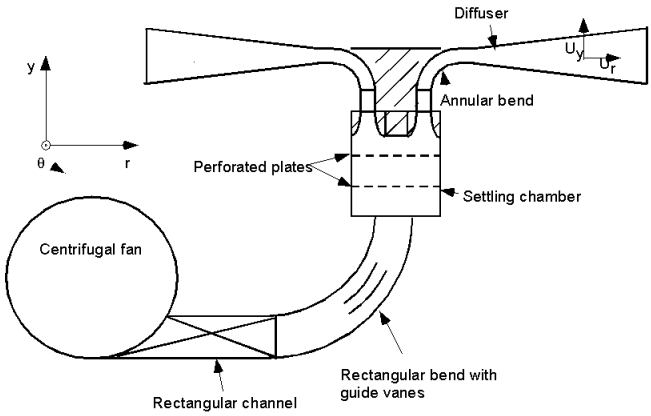

Figure 1: The figure shows the cross section when slicing the rig along the *y* axis.

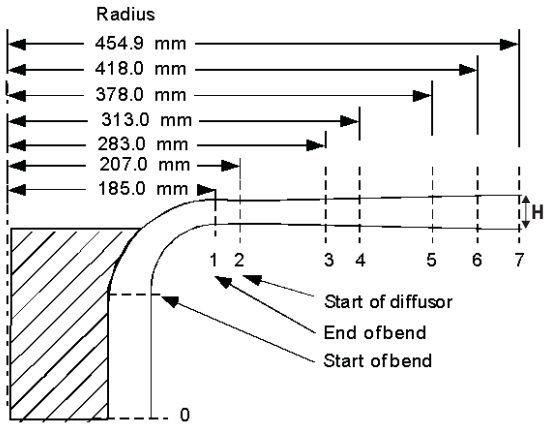

Figure 2: The figure shows an axisymmetric cross section of the model. The radial cross sections where the velocity was measured and skin-friction were measured and calculated are represented by the dashed lines(Number 1- 7).

Numerical model

The numerical calculations were performed with the FLUENT code version 6.0 [2]. The code has several turbulence models incorporated and is easy to use. The numerical domain was identical to the geometry shown in Figure 2, and was modeled as being axisymmetric. Uniform mean velocity was set at section

Sec.	y_c	r_c	H	$\|\overline{U}\|$	Re_{Dh}
#	$[mm]$	$[mm]$	$[mm]$	$[m/s]$	-
0	0	108.7	38.0	27.0	8.0×10^4
1	284.0	184.8	22.3	27.0	8.0×10^4
2	284.0	207.1	20.0	26.9	7.2×10^4
3	284.0	283.0	23.3	16.9	5.2×10^4
4	284.0	313.0	24.6	14.5	4.7×10^4
5	284.0	378.0	27.5	10.7	3.9×10^4
6	284.0	418.0	29.3	9.1	3.5×10^4
7	284.0	454.9	31.0	7.9	3.3×10^4

Table 1: Details of the geometry. y_c and r_c denote the position of the geometrical centerline at each of the dashed lines shown in figure 2. $D_h = 2H$ is the hydraulic diameter and Re_{Dh} is the bulk flow Reynolds number.

0. This is close to the experimental conditions since a strong contraction upstream of section 0 in the experiment produced a nearly uniform velocity profile with very thin boundary layers. In agreement with observations from the experiment, the static pressure at the outlet was set to be uniform. At the walls the no slip condition was imposed. The grid was made up of 80×660 quadrilateral cells in the wall normal and streamwise direction respectively, and grid independence was checked with two additional grids of 70×472 and 50×660 resolution. No major discrepancy was found in velocity and skinfriction between these three grids[7]. Towards the wall both the equilibrium and non-equilibrium law of the wall approach was found inadequate [7]. The first grid point was therefore placed well within the viscous sublayer ($y^+ < 5$) and a two layer model was chosen. In the viscosity affected region, $Re_y = \rho y\sqrt{k}/\mu < 200$, the one equation model of Wolfstein [10] was used. In the fully turbulent region several turbulence models with a varying degree of complexity were employed ranging from the one-equation model of Spalart-Allmaras[8] to the Reynolds stress model given by Launder [4]. In the mid range complexity the two equation $k-\varepsilon$-models of Launder and Sharma [5], often referred to as the standard $k-\varepsilon$ model (std), the "renormalization group" (RNG) [1], and the realizable $k-\varepsilon$ (Realz) model by Shih et al. [6] were used. In the buffer layer the turbulent viscosity was estimated with a blending function between the values calculated in the inner and outer regions [3]. Further details concerning the numerical code and turbulence models may be found in reference [2].

Static Pressure

Static pressure was measured along radially directed planes, at the hub and boss surfaces (Figure 3). The static pressure recovery coefficient $C_p(s) = (P(s) - P_{in})/\overline{q}_{in}$ quantify how much of the kinetic energy is recovered as static pressure energy, P, downstream the channel. s is the streamwise length measured from the first static pressure hole which was located $100mm$ downstream of section 0 in figure 2. $q_{in} = 1/2\rho|U|^2$ is the kinetic energy of the mean flow, with velocity U and density ρ, at $s = 0$. Figures 4 and 5 show comparisons between the measured, and calculated pressure recovery coefficient. The dotted vertical lines are the borders between the different zones of the configuration. 1) Inlet annular pipe, 2) Axial-Radial bend, 3) Stabilizer, and 4) Diffuser. As can be seen from the figure there is a reasonable degree of collapse between the computed, and the measured pressure distribution. Following the hub side surface the agreement is considered very good. There is a small deviation at the lower peak of C_p in the bend of about 5%. Along the boss side the agreement is also good although the relative deviation in the bend is considerably larger. With respect to the

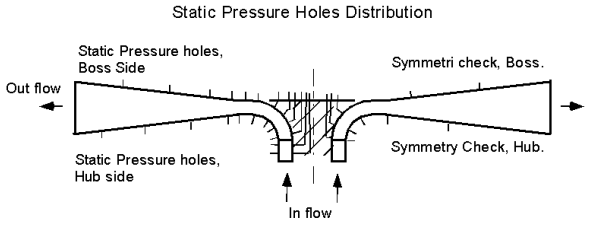

Figure 3: Distribution of static pressure holes (ry-plane of diffuser). The holes denoted as "Symmetric check" were only used in documenting the axisymmetry of the static pressure distribution.

form of the curves the agreement is good along both walls. Local peaks and abrupt changes in gradients coincide well with respect to the flow distance s. It is also to be noted that a small difference between the geometry used in the CFD, and the real geometry could result in discrepancies, especially in the narrowest regions of the flow. Table 2 gives a comparison of C_p at the diffuser outlet. As seen from the table all methods are within 5% of the experimentally obtained value with the RSM model being the closest.

Method	C_p	$(C_{p,cfd} - C_{p,exp})/C_{p,exp}$in%
Exp.	0.678	0
SA	0.6566	-3.2
$k-\varepsilon_{std}$	0.7082	4.4
$k-\varepsilon_{RNG}$	0.6986	3.0
$k-\varepsilon_{realz}$	0.7054	4.0
RSM	0.6754	-0.4

Table 2: Comparisons of calculated and experimentally obtained pressure recovery at the diffuser outlet.

Mean velocity

Figures 6 and 7 shows a comparison of calculated versus measured data of the normalized radial mean velocity component at the outlet of the bend (r185), and close to the outlet of the diffuser (r455). We clearly see that the choice of turbulence model results in largely deviating profiles. At r185 the $k-\varepsilon_{std}$ results in completely erroneous profiles indicating the peak of the velocity profile to be at the opposite side of the channel compared to the experimental results. The SA, $k-\varepsilon_{RNG}$ and $k-\varepsilon_{realz}$ represent the velocity profiles well while the RSM model performs less well. At the hub side we clearly see a large difference between the gradient of the RSM model and the experimental results. The RSM model also has some abnormal behavior at $y/H \approx 0.7$ where it takes a distinct dip when approaching the wall. At r455 the SA model wrongly indicate a separation zone at the outlet and generally compare poorly with the measured profile. Among the two equation models we clearly see that the $k-\varepsilon_{RNG}$ and the $k-\varepsilon_{realz}$ models are in better agreement with the experimental data than the other models. Both these models estimate the velocity peak with reasonable accuracy and also the velocity descent from the peak towards the wall. The $k-\varepsilon_{realz}$ model clearly match the data best as seen when approaching the walls (especially at the hub side). Somewhat surprisingly the RSM model does not represent the current flow very well. It is more in error with respect to the experimental data than the $k-\varepsilon_{RNG}$ and the $k-\varepsilon_{realz}$ models. This is seen especially at the hub side wall where it overestimates the velocity largely and completely misses on the velocity gradient in the vicinity of the wall. The explanation for the rather poor behavior of the RSM model is for the time being not clear.

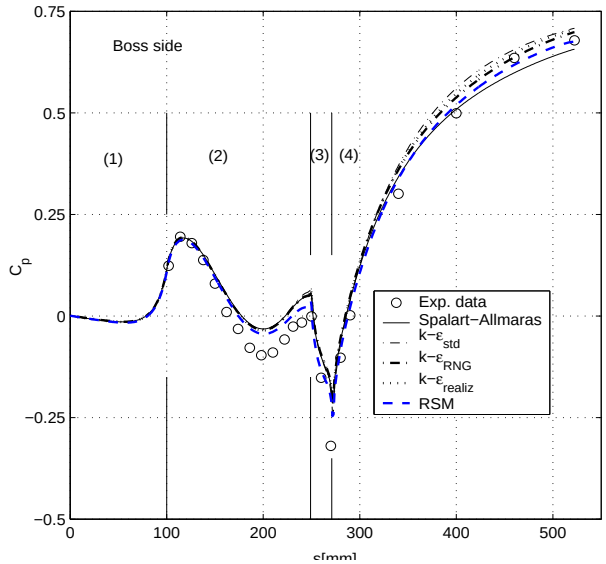

Figure 4: Comparison of experimental, and computed Cp values along the boss surface.

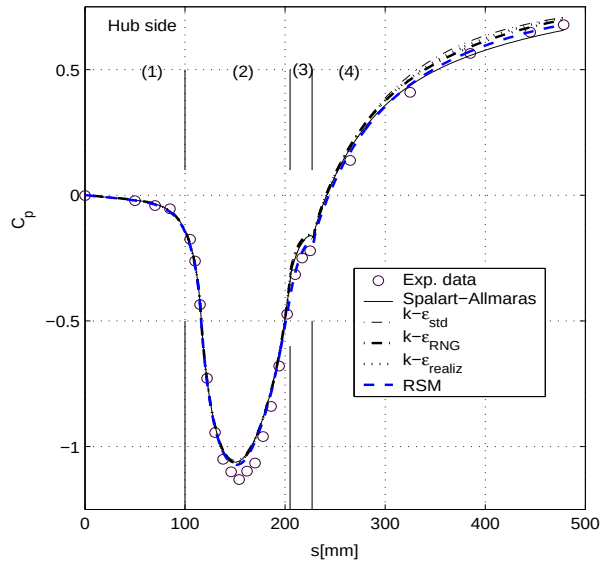

Figure 5: Comparison of experimental, and computed Cp values along the hub surface.

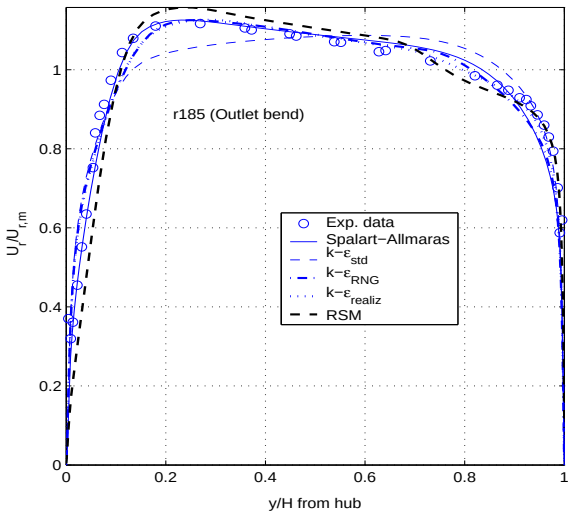

Figure 6: Calculated and measured U_r mean velocity at r185.

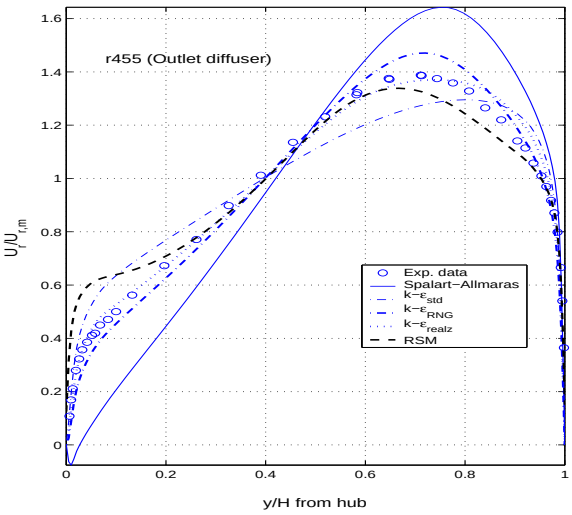

Figure 7: Calculated and measured U_r mean velocity at r455.

Skin-friction

Due to the difficulty in accurately estimating the experimental skin-friction for the current flow three different methods were employed. The methods used were velocity fitting using the Musker-Granville function, dynamic head pressure measurements using a $0.9mm$ diameter Preston tube, and the Von-Kárman momentum equation based correlation of White[9]. Figure 8 and Figure 9 show the comparison of the globally normalized skin-friction coefficient, $C_f = 2\tau_w/\rho U_{r,in}^2$, at the hub and boss sides respectively. At the hub side, in the diffuser, the three experimental based methods agree very well in the outer part, but are more scattered in the inner part of the diffuser. The simulation results however are scattered throughout most of the domain. The RSM model indicates a significantly higher C_f than the other models while the SA model is the lowest and predicts separation at $r \approx 275mm$. The $k-\varepsilon_{RNG}$ and the $k-\varepsilon_{realz}$ models agree well with each other but underpredict the experimental C_f towards the outlet. The $k-\varepsilon_{RNG}$ simulation is very close to separation at the hub side as we see from the included subfigure in Figure 8. The $k-\varepsilon_{std}$, fits the experimental data best through the diffuser. At the boss side the experimentally based methods are less scattered and the agreement between simulations and the experiment is considerably better. At this side both the $k-\varepsilon_{std}$ and RSM model overpredicts the skin-friction slightly. The SA model underpredicts the C_f in the beginning of the diffuser but decays less rapidly compared to the other models and ends up overpredicting the C_f at the outlet. The $k-\varepsilon_{RNG}$ and the $k-\varepsilon_{realz}$ models agree very well with the experiments.

The two first measurements in the figures are in the vicinity of the borders between the bend-stabilizer and stabilizer-diffuser respectively. At these positions C_f exhibits a discontinuous be-

havior due to the discontinuity in the gradient of the width with respect to the streamwise distance. In this region a small positioning error in the streamwise direction leads to large errors in C_f. Hence it is difficult to compare the experimental and computed distributions here. However, it appears that the experimental values lie within the ranges of the CFD values.

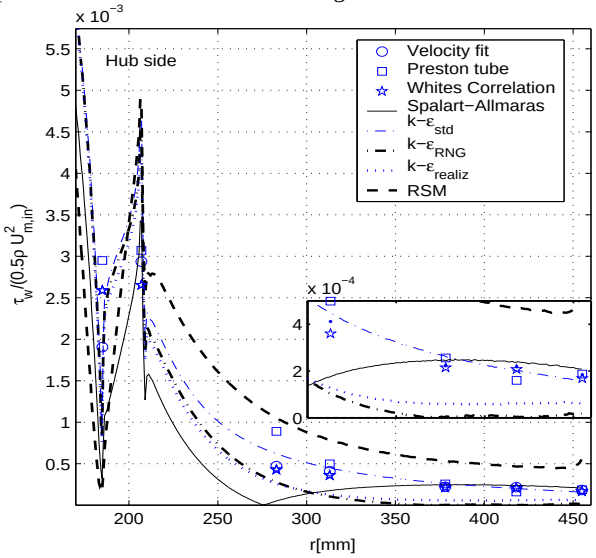

Figure 8: Comparison between calculated and experimentally obtained estimates of the skin-friction coefficient at the hub side of the channel.

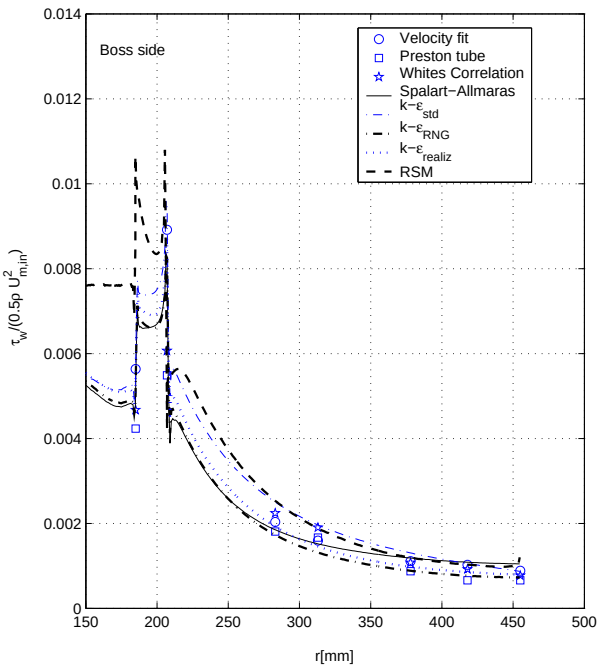

Figure 9: Comparison between calculated and experimentally obtained estimates of the skin-friction coefficient at the boss side of the channel.

Summary

The current work describes the flow in an axial to radial bend-diffuser configuration. This configuration is used as a pressure recovery device behind axial compressors when axial space is limited. No prior reports on this particular flow configuration has been found. Radial diffusers are not uncommon, but normally there is a centrifugal compressor upstream of the diffuser. Mean velocity and static pressure has been measured and based on these data the skin-friction, C_f, has been calculated. The experimental data have been compared with numerical simulations using the Fluent software package. The comparisons show that with respect to the pressure recovery, C_p, the differences between the measured and calculated data are within 5%. The one equation turbulence model underestimates while the two equation models overestimate the measured value. The Reynolds stress model (RSM) agrees with the measurements to within 1%. The realizable $k-\varepsilon$ model, closely followed by the renormalized group model (RNG), clearly predicted the mean velocity best while the other models did not compare very well. Skin friction was predicted fairly well along the boss side surface while being less accurate along the hub surface. The one equation model incorrectly predicts a small separation zone along the hub side surface. A detailed investigation of the different turbulence models clarifying what causes the large differences in especially C_f and U_r has not been carried out yet.

References

[1] Choudhury, D., Introduction to the renormalization group method and turbulence modeling, Technical Report TM-107, Fluent Inc. Technical Memorandum, 1993.

[2] Fluent Incorporated, Holmworth House, Corthworth Road, Sheffield, S11 9LP, UK, *Fluent 6.1 Users Guide*, 2003.

[3] Jongen, T., *Simulation and Modeling of Turbulent Incompressible Flows*, Ph.D. thesis, EPF Lausanne, Switzerland, 1992.

[4] Launder, B., Reece, G. and Rodi, W., Progress in the development of a reynolds-stress turbulence closure., *J. Fluid Mech*, **68**, 1975, 537–566.

[5] Launder, B. and Sharma, D., *Lectures in Mathematical Models of Turbulence*, Academic Press, London, England, 1972.

[6] Shih, T., Liou, W., Shabbir, A. and Zhu, J., A new k- eddy-viscosity model for high reynolds number turbulent flows - model development and validation., *Computers Fluids*, **24**, 1995, 227–238.

[7] Simonsen, A., *Experimental and numerical investigation of a bend diffuser configuration*, Ph.D. thesis, Department of Energy and Process Engineering, The Norwegian University of Science and Technology, Trondheim, Norway, 2003.

[8] Spalart, P. and Allmaras, S., A one-equation turbulence model for aerodynamic flows., *AIAA*, **0439**.

[9] White, F., *Viscous fluid flow*, McGraw-Hill, 1991, second edition.

[10] Wolfstein, M., The velocity and temperature distribution of one-dimensional flow with turbulence augmentation and pressure gradient, *Int. J. Heat Mass Transfer*, **12**, 1969, 301–318.